Biomechanical Evaluation of Different Balloon Positions for Proximal Optimization Technique in Left Main Bifurcation Stenting

Accepted manuscript at https://doi.org/10.1016/j.carrev.2020.05.028

Biomechanical Evaluation of Different Balloon Positions for Proximal Optimization Technique in Left Main Bifurcation Stenting

Running Title: Proximal Optimization technique in Left Main bifurcation

Gianluca Rigatelli[1], Marco Zuin[1,2], Claudio Chiastra[3], Francesco Burzotta[4]

1 Cardiovascular Diagnosis and Endoluminal Interventions Unit, Rovigo General Hospital, Rovigo, Italy

2 University of Ferrara, School of Medicine, Ferrara, Italy

3 PoliTo[BIO]Med Lab, Department of Mechanical and Aerospace Engineering, Politecnico di Torino, Turin, Italy

4 Fondazione Policlinico Universitario A, Gemelli IRCCS, Università Cattolica del Sacro Cuore, Rome, Italy

*The authors equally contribute to the manuscript

Type of Article: Original research

Conflict of interest: None of the authors have conflict of interest to declare

For Correspondence:

Prof. Gianluca Rigatelli MD, FACP, FACC, FESC, FSCAI

Cardiovascular Diagnosis and Endoluminal Interventions,

Rovigo General Hospital, Viale Tre Martiri, 45100, Rovigo, Italy

Phone: +3903471912016; Fax: +390425394513;

e-mail: jackyheart@libero.it

Abstract

Background

Proximal optimization technique (POT) is a key step during left main (LM) bifurcation stenting. However, after crossover stenting, the ideal position of POT balloon is unclear. We sought to evaluate the biomechanical impact of different POT balloon positions during LM cross-over stenting procedure.

Methods

We reconstructed the patient-specific LM bifurcation anatomy, using coronary computed tomography angiography data of 5 consecutive patients (3 males, mean age 66.3 ± 21.6 years) with complex LM bifurcation disease, defined as Medina 1,1,1, evaluated between 1st January 2018 to 1st June 2018 at our center. Finite element analyses were carried out to virtually perform the stenting procedure. POT was virtually performed in a mid (marker just at the carina cut plane), proximal (distal marker 1 mm before the carina) and distal (distal marker 1 mm after the carina) position in each investigated case. Final left circumflex obstruction (SBO%), strut malapposition, elliptical ratio and stent malapposition were evaluated.

Results

The use of both proximal and distal POT resulted in a smaller LM diameter compared to the mid POT. SBO was significantly higher in both proximal and distal configurations compared to mid POT: 38.3 ± 5.1 and 29.3 ± 3.1 versus 18.3 ± 3.6%, respectively. Similarly stent malapposition was higher in both proximal and distal configurations compared to mid POT: 1.3 ± 0.4 and 0.82 ± 1.8 versus 0.78 ± 1.2, respectively.

Conclusions

Mid POT offers the best results in terms of LCx opening maintaining slightly smaller but still acceptable LM and LAD diameters compared to alternative POT configuration.

Key words: Bifurcations, Left main, POT

1. Introduction

Single stent implantation (also called “provisional technique”) is currently the preferred technique for percutaneous coronary interventions on the majority of unprotected left main (LM) bifurcations [1]. According to the best practices for provisional technique in LM, a stent sized according to the left anterior descending artery is usually implanted from LM to left anterior descending (“crossover” stenting) and LM dilation with appropriately sized balloon is used to optimize stent expansion and expansion. Such critical step, called proximal optimization technique (POT) has been proved to correct both the proximal main vessel (MV) malapposition and optimize the side branch (SB) ostium strut opening for proper wire re-crossing into the distal cell [2,3]. In the setting of major size mismatch (like often in LM bifurcation), POT might be crucial step and may warrant improved long-term clinical outcomes [4]. When performing POT, theoretically, balloon position may influence procedural efficacy. Thus, we performed a virtual stenting study [5,6], aimed to evaluate the biomechanical impact of different balloon positions for POT in patients with LM bifurcation disease.

2. Methods

2.1. Patient selection

We reconstructed the patient-specific coronary bifurcation anatomy using the coronary computed tomography angiography (CCTA) data of consecutive patients affected by complex LM bifurcation disease evaluated between 1st January 2018 to 1st June 2018 at the section of Cardiovascular diagnosis and endoluminal interventions of Rovigo General Hospital, Italy.

Inclusion criteria were patients aged ≥18 years old with severe unprotected LM bifurcation disease assessed by both CCTA and then by coronary angiography (CA). Specifically, unprotected complex LM bifurcation disease was defined as: (1) a stenosis with a diameter of >50% involving the mid-

shaft/distal main vessel with significant involvement (>50% luminal narrowing and >10 mm length by visual estimation) of the left anterior descending coronary artery (LAD) and left circumflex artery ostia (diameter >2.5 mm by visual estimation) and, (2) without any patent graft to the left anterior descending artery or left circumflex artery. Written informed consent for the CCTA and CA was obtained from all patients and the local Board approved the study.

2.2. Coronary computed tomography angiography

CCTA was acquired using a 64-slice multi-detector computed tomography scanner (64-detector row Lightspeed VCT scanner, GE Healthcare, Milwaukee, WI, USA). Per our institution protocol, before the imaging acquisition, patients were pre-treated with oral and/or intravenous beta-blockers, as necessary, to achieve a target resting heart rate (HR) < 70 beats/min. Electrocardiographic (ECG) gating was used for all scans. The scanning protocol was adjusted for patient weight and heart rate (HR). A bolus intravenous dose of iodine contrast was given through the basilic or cephalic vein. The entire volume of the heart was acquired in 8–9 s during a single breath-hold. Each examination was independently interpreted by a trained CT radiologist using a combination of axial images, 3D volume-rendered images, multiplanar reformations, and maximum intensity projections.

2.3. Coronary angiography

CA was performed using a 6F radial approach. Angiographic data were reviewed by a 20 years-experienced angiographic operator (G.R.). Discordances between CCTA and CA results were resolved via collegial discussion with the CT radiologist. Quantitative coronary angiography (QCA) estimation (CAAS II 5.0 version; Pie Medical, Maastricht, The Netherlands) was used to quantify the coronary artery disease on CA while the type of bifurcation lesion was defined according to the Medina classification [7]. Lesion characteristics have been evaluated following current classifications which can be found in Sianos et al. [8].

2.4. Coronary bifurcation models

Five patient-specific vessel geometries of complex LM bifurcation were investigated.

The bifurcation geometries were reconstructed using the open-source software package VMTK (Vascular Modeling Toolkit, http://www.vmtk.org), identifying the MV vessel centerline and then splitting the branches of the bifurcation (Fig. 1). In a second step, external wall surfaces were created with circumferential cross sections perpendicular to the centerlines using the computed-aided design software Rhinoceros 4.0 Evaluation (McNeel & Associates, Indianapolis, IN, USA). Atherosclerotic plaques were modeled considering the distance between each node and the centerline of the luminal surface. The reconstructed vessel's wall consisted of three layers with realistic material properties of the coronary artery while the atherosclerotic plaque was modeled based on CT findings as lipid with a 4 mm long half-calcified ring distal to the carina. Specifically, the material properties of the plaque constituents were modeled in accordance with Holzapfel et al. [9] and Loree et al. [10] . Specifically, we assumed a combination of fibrous tissue (α = 5%), lipid (β = 20%) and calcium (γ = 75%) as components for a homogenous calcification agglomerate. Fibrous and calcium material properties were taken from experimental tests on human atherosclerotic tissues [10], while the lipid was modeled as a very soft material [11].

Coronary artery stenosis (Diameter Stenosis %) and minimal lumen area were calculated considering the reconstructed coronary artery models. Specifically, the severity of the stenosis was computed as 100% minus the percentage of minimal lumen area to the reference lumen area [12].

2.5. Virtual stenting

Finite element analyses were performed to virtually deploy and post-dilate stents and balloons. We assumed that after stent deployment and implantation, both in the MB and SBs, there was no residual stenosis. The simulated coronary stent resembles the strut design and linkage pattern of the Orsiro stent (Biotronik IC, Bulack, Switzerland) and was generated by reverse-engineering using

high-resolution micro-computed tomography imaging. The Orsiro stent presents ultrathin struts (60 μm up to 3.0 mm diameter stent and 80 mm up to 4.0 mm stent). Moreover, this stent is made of a Co-Cr alloy and its material properties were taken from Schmidt et al. [13]. To keep the analysis runtime reasonable, a finite element mesh consisting of 17,280 elements was used for the Orsiro stent.

The virtual stenting procedure was performed using the ANSYS (ANSYS Inc., Cannonsburg, MI, USA) finite element solver by following a similar approach as reported in previous virtual bench test studies [[14], [15], [16], [17]].The common cross-over stenting technique was virtually replicated as follows:

1. Wiring of both branches: LAD and LCx;
2. Predilation with semi-compliant balloon (Euphora 3.0 × 15 mm, (Medtronic Ireland, Galway, Ireland)) matching the distal reference diameter at nominal pressure;
3. Stenting of MV with stent diameter according to the distal MV reference diameter as currently recommended;
4. POT with a non-compliant balloon (4.0 × 8 mm) at nominal pressure, matching 1:1 the proximal MV reference diameter.

2.6. Virtual final proximal optimization techniques (POT)

The balloon-tipped catheter consisted of a guide wire, a catheter shaft and a folded non-compliant balloon. The radio-opaque markers were reconstructed as well to ensure an adequate position of the marker for the final POT. The balloon material model was a classical one based on Hooke's theory of elasticity with Young's modulus E = 900 MPa and Poisson's ratio ν = 0.3 [18]. Moreover, the free expansion of the Euphora balloon was simulated and validated through the comparison with the manufacturer's compliance chart.

Specifically, in each procedure, the POT was performed to the virtual distal shoulder position (balloon parallelism loss) relative to the carina cut plane (Fig. 1) and defined as follows:

- Proximal, when the distal marker was 1 mm before the carina;
- Standard, when the distal marker was just at the carina cut plane;
- Distal, when the distal marker was 1 mm after the carina.

2.7. Biomechanical analysis

The cross-sectional lumen area (mm^2), and the mean (D_{mean}), maximum (D_{max}) and minimum (D_{min}) lumen diameters were measured using an adequate planar projection from the bifurcation 3D reconstruction. Moreover, the final SB obstruction (SBO) was calculated by planimetry on 3D reconstruction as (A_1/A_2) × 100% (A_1 = total strut area in ostium; A_2 = total ostium area). The elliptical ratio was calculated as D_{max}/D_{min} (1.0 = perfect circularity). Finally, stent malapposition was calculated by cross-sectional stent analysis as percentage of malapposed/total struts.

2.8. Statistical analysis

Continues variables were expressed as mean ± standard deviation (SD) and were compared by Student's *t*-test if the data had normal distribution, otherwise by Wilcoxon-Mann-Whitney *U* test. The comparison between the different stent deformations across the three POT positions was evaluated using ANOVA with Bonferroni post hoc analysis. Statistical significance was defined as $p < 0.05$. Statistical analyses were performed using SPSS package version 20.0 (SPSS, Chicago, IL, USA).

3. Results

3.1. Patient and lesion characteristics

CCTA and CA records of 5 patients (3 males, mean age 66.3 ± 21.6 years) were used for the analysis: LM bifurcation disease was classified as Medina 1,1,1. The mean carina angle of the bifurcations was 70.1.3 ± 12.56° measured using an electronic goniometer.

On CA, calcification was classified as moderate in 4 cases and mild in 1 cases whereas lesion type was B in 2 cases and C in 3 cases. The stenoses involving the LM, LAD and LCX ostia were 83.2 ± 6.5%, 85.2 ± 2.2% and 82.5 ± 3.1%, respectively. Mean length of the disease was calculated as 23.6 ± 8.7 mm. The LM lesion length was 12.1 ± 3.1 mm while LAD and LCx lesion lengths were 11.5 ± 2.2 mm and 12.1 ± 2.5 mm, respectively. At baseline, the minimum lumen diameter was 1.7 ± 1.4 mm in LM, 1.3 ± 0.5 mm in LAD and 1.1 ± 1.2 mm in LCx.

3.2. Final mean lumen diameters after POT

Table 1 reports the results of the biomechanical analysis. Both proximal and distal POT resulted in a slightly smaller LM diameter than traditional POT, whereas the LAD diameter was bigger in LAD with distal POT compared to proximal and traditional configurations. Regarding LCx, the lumen diameters were smaller in both proximal and distal POT compared to traditional technique.

3.3. Side branch obstruction and elliptical ratio

Table 2 shows the SBO and stent malapposition which were significantly higher in both alternative configurations compared to standard POT ($p < 0.05$) (Fig. 2). The elliptical ratio was in favor of traditional POT in all segments of the bifurcation, in particular at the carina: 0.75 ± 0.04 in standard POT versus 0.60 ± 0.03 and 0.80 ± 0.02 in proximal and distal POT configurations, respectively. However, in the distal POT configuration the elliptical ratio resulted lower than in the proximal one, with similar values with respect of the traditional POT.

4. Discussion

Our virtual bench study suggests that POT performed placing the distal balloon marker just at the carina cut plane is more effective than the alternative POT configurations (i.e. proximal and distal POT) in terms of SBO and elliptical ratio.

In the past, the classic final kissing balloon inflation constituted the "mantra" of the interventional cardiologist in the optimization of LM stenting [19]. More recently, the POT and its modified techniques such as the POT-Side-POT or *Re*-POT, showed potential of correcting the kissing balloon inflation drawbacks while achieving a great ostial opening for the SB [20]. Several bench and clinical studies showed that kissing balloon inflation restores the MV stent volume, area, and symmetry loss after SB dilation in the bifurcation segment at the cost of some zones of strut malapposition and a certain proximal elliptical deformation [[21], [22], [23]]. On the contrary, POT promotes full proximal stent apposition and confers a more natural circular shape to the proximal segment of the MV [24]. POT also increases the size of opening of the SB ostium and, by that, facilitates a distal wire recrossing, independently of which stent type is used [25]. These features result particularly attractive when dealing with large and important bifurcation such as the LM; indeed, because of the amount of jeopardize myocardium, the maintenance of a sufficient opening of the LCx is crucial for long-term outcomes. Decreasing malapposition in LM in particular seems of a certain importance being stent malapposition one of the numerous determinants of stent thrombosis [26,27].

In this particular setting, virtual bench testing allows for evaluating the impact of different interventional maneuvers in an ideal identical vascular bifurcation and to study the impact of these maneuvers on different stent configurations and anatomical structures such as the LM carina. As matter of fact, in vitro bench testing and 3-priting models have the advantage of providing a realistic assessment of both bifurcation geometry and stent properties. Unfortunately, these approaches cannot simulate the elastic properties of the coronary artery as well as an accurate reconstruction of atherosclerotic plaque in term of luminal stenosis, plaque burden, and wall calcification. Moreover, they allow only a "static" analysis being unbale to replicate the coronary artery motion and deformations during the cardiac cycle making impossible the assessment of strut deformations with increasing inflation pressure over the time. Moreover, these approaches require the use of micro-CT imaging for the analysis which is related with significant costs and limited

availability [6,[28], [29], [30]]. Conversely, our approach allows an accurate dynamic reconstruction of the patient-specific 3D coronary artery geometry modeling the plaque and the bifurcation geometry in more realistic manners with lower costs and resources [30].

A setting completely different from the one used by Derimay et al. [31], who recently explored the effect of different position for POT in a bench fractal model quantifying the results with 2D- and 3D-OCT. In their study a Synergy™ stent (Boston Scientific, USA) was implanted on left-main fractal bench models. Initial POT was performed in 3 positions according to distal shoulder position relative to the carina cut plane very similarly with our study: 1) "proximal", 1 mm before carina; 2) "medium", just at carina; 3) "distal", 1 mm after carina. Although initial POT improved malapposition in all positions, the residual malapposition was greater in "proximal" position which also failed to improve side-branch obstruction, unlike "medium" or "distal" POT. Conversely, "distal" POT significantly overstretched the main-branch ostium. They concluded that the best position is just at the carina cut plane ("medium").

While Derimay et al. used a bench fractal model which per se has the limitation to be a pure bench model with limited correlation with in vivo- clinical setting, our study used the reconstruction of a patient's specific bifurcation model with real plaque distribution and composition, a setting which could approximate the real clinical situation. Proximal POT in both studies resulted in a higher malapposition and SBO but differently from Derimay, our study observed that distal POT is definitively better of proximal POT in term of SBO, elliptical ration and final diameters of LAD and LCX. However the conclusions reached by both studies are similar and indirectly confirmed that biomechanical patients specific model reconstruction based on CT offers an accuracy comparable to traditional bench studies in term of biomechanical deformation, providing a setting closer to clinical "real world" pictures.

The results of our study rise some considerations: firstly, the original site for POT represents an efficient site from a biomechanical viewpoint, allowing a good LCx opening which, in turn, enables to avoid the use of kissing balloon inflation; secondly, when POT is performed inadvertently more

proximally, the sequence POT-side-POT or *Re*-POT is probably the best way to restore LCx opening, deflecting the malapposed struts towards the LCx ostium; thirdly, when the POT is performed more distally, the SBO is significantly worse but the LAD and LM lumen diameter are even larger than after traditional POT.

4.1. Limitations

Our study has some limitations. Firstly, the study design is retrospective and monocentric. Secondly, the number of patients evaluated is small. Since the outcome of both stent implantation and biomechanical analyses strictly depends on the quality of geometrical data, model reconstruction and boundary conditions, our patient-specific 3D segmentation reconstruction and virtual stent implantation allowed us to minimize the potential drawbacks related to the sample size. Thirdly, different plaques configurations (fully lipid or fibrous), which have not been tested in our study, might led to different results. Lastly, further traditional bench studies with micro-CT evaluation and possibly clinical OCT validated studies are necessary to confirm our preliminary results, also using different stent and balloon designs.

5. Conclusions

Biomechanically, in complex LM bifurcation, POT performed with the balloon marker just at the carina cut plane offers the best results in terms of SBO and LCx opening maintaining slightly smaller but still good LM and LAD lumen diameters compared to more proximal or distal POT configurations. Additional optimizations would be necessary when POT is performed proximally for the high rate of stent malapposition and SBO.

CRediT authorship contribution statement

Gianluca Rigatelli: Conceptualization, Methodology, Software, Data curation, Writing - original draft, Writing - review & editing, Supervision. **Marco Zuin:** Conceptualization, Software, Writing - original draft. **Claudio Chiastra:** Data curation, Software, Writing - review & editing, Visualization. **Francesco Burzotta:** Writing - review & editing.

Declaration of competing interest

Gianluca Rigatelli, Marco Zuin and Claudio Chiastra have no conflict of interest to declare.

Francesco Burzotta reports to have received speaker's fee from Medtronic. Abbott, Abiomed.

References

[1]

F. Burzotta, J.F. Lassen, A.P. Banning, T. Lefèvre, D. Hildick-Smith, A. Chieffo, *et al.***Percutaneous coronary intervention in left main coronary artery disease: the 13th consensus document from the European Bifurcation Club**

EuroIntervention, 14 (2018), pp. 112-120

[2]

T. Rab, I. Sheiban, Y. Louvard, F.J. Sawaya, J.J. Zhang, S.L. Chen**Current interventions for the left main bifurcation**

JACC Cardiovasc Interv, 10 (2017), pp. 849-865

[3]

Finet G, Derimay F, Motreff P, Guerin P, Pilet P, Ohayon J, Darremont O, Rioufol G. Comparative analysis of sequential proximal optimizing technique versus kissing balloon inflation technique in provisional bifurcation stenting: Fractal Coronary Bifurcation Bench Test. JACC CardiovascInterv. 2015 8:1308-17.

[4]

G. Rigatelli, M. Zuin, K. Karamfilof, D. Cavazzini, G. Braggion, S. Perilli, *et al.***Impact of different final optimization techniques on long-term clinical outcomes of left main cross-over stenting**

Cardiovasc Revasc Med, 20 (2019), pp. 108-112

[5]

A.P. Antoniadis, P. Mortier, G. Kassab, G. Dubini, N. Foin, Y. Murasato, *et al.***Biomechanical modeling to improve coronary artery bifurcation stenting: expert review document on techniques and clinical implementation**

JACC Cardiovasc Interv, 8 (2015), pp. 1281-1296

[6]

F. Migliavacca, C. Chiastra, Y.S. Chatzizisis, G. Dubini**Virtual bench testing to study coronary bifurcation stenting**

EuroIntervention., 11 (2015), pp. V31-V34

[7]

A. Medina, J. Suarez de Lezo, M. Pan**A new classification of coronary bifurcation lesions**

Rev EspCardiol, 59 (2006), p. 183

[8]

G. Sianos, M.A. Morel, A.P. Kappetein, M.C. Morice, A. Colombo, K. Dawkins, *et al.***The SYNTAX score: an angiographic tool grading the complexity of coronary artery disease**

Eurointervention, 1 (2005), pp. 219-227

[9]

G. Holzapfel, G. Sommer, C.T. Gasser, P. Regitnig**Determination of layer- specific mechanical properties of human coronary arteries with nonatherosclerotic intimal thickening and related constitutive modeling**

Am J Physiol Heart Circ Physiol, 289 (2005), pp. H2048-H2058

[10]

H.M. Loree, A.J. Grodzinsky, S.Y. Park, L.J. Gibson, R.T. Lee**Static circumferential tangential modulus of human atherosclerotic tissue**

J Biomech, 27 (1994), pp. 195-204

[11]

G.C. Cheng, H.M. Loree, R.D. Kamm, M.C. Fishbein, R.T. Lee**Distribution of circumferential stress in ruptured and stable atherosclerotic lesions. A structural analysis with histopathological correlation**

Circulation, 87 (1993), pp. 1179-1187

[12]

M. Zuin, G. Rigatelli, D. Vassilev, F. Ronco, A. Rigatelli, L. Roncon**Computational fluid dynamic-derived wall shear stress of non-significant left main bifurcation disease may predict acute vessel thrombosis at 3-year follow-up**

Heart Vessels, 35 (2020), pp. 297-306

[13]

W. Schmidt, P. Lanzer, P. Behrens**Direct comparison of coronary bare metal vs. drug-eluting stents: same platform, different mechanics?**

Eur J Med Res, 23 (2) (2018)

[14]

F. Iannaccone, C. Chiastra, A. Karanasos, F. Migliavacca, F.J.H. Gijsen, P. Segers, *et al.***Impact of plaque type and side branch geometry on side branch compromise after provisional stent implantation: a simulation study**

EuroIntervention., 13 (2017), pp. e236-e245

[15]

P. Mortier, Y. Hikichi, N. Foin, G. De Santis, P. Segers, B. Verhegghe, *et al.***Provisional stenting of coronary bifurcations: insights into final kissing balloon post-dilation and stent design by computational modeling**

JACC Cardiovasc Interv, 7 (2014), pp. 325-333

[16]

P.D. Morris, J. Iqbal, C. Chiastra, W. Wu, F. Migliavacca, J.P. Gunn**Simultaneous kissing stents to treat unprotected left main stem coronary artery bifurcation disease; stent expansion, vessel injury, hemodynamics, tissue healing, restenosis, and repeat revascularization**

Catheter Cardiovasc Interv, 92 (2018), pp. E381-E392

[17]

M.J. Grundeken, C. Chiastra, W. Wu, J.J. Wykrzykowska, R.J. De Winter, G. Dubini, *et al.***Differences in rotational positioning and subsequent distal main branch rewiring of the Tryton stent: an optical coherence tomography and computational study**

Catheter Cardiovasc Interv, 92 (2018), pp. 897-906

[18]

F. Gervaso, C. Capelli, L. Petrini, S. Lattanzio, L. Di Virgilio, F. Migliavacca**On the effects of different strategies in modelling balloon-expandable stenting by means of finite element method**

J Biomech, 41 (2008), pp. 1206-1212

[19]

M. Zhong, B. Tang, Q. Zhao, J. Cheng, Q. Jin, S. Fu**Should kissing balloon inflation .after main vessel stenting be routine in the one-stent approach? A systematic review and meta-analysis of randomized trials**

PLoS One, 13 (2018), Article e0197580

[20]

F. Derimay, G. Souteyrand, P. Motreff, P. Guerin, P. Pilet, J. Ohayon, *et al.***Sequential proximal optimizing technique in provisional bifurcation stenting with everolimus-eluting bioresorbable vascular scaffold: Fractal Coronary Bifurcation Bench for Comparative Test between absorb and XIENCE Xpedition**

JACC Cardiovasc Interv, 9 (2016), pp. 1397-1406

[21]

N. Foin, R. Torii, P. Mortier, M. De Beule, N. Viceconte, P.H. Chan, *et al.***Kissing balloon or sequential dilation of the side branch and main vessel for provisional stenting of bifurcations: lessons from micro-computed tomography and computational simulations**

JACC Cardiovasc Interv, 5 (2012), pp. 47-56

[22]

Iwasaki K. MurasatoY, T. Yamamoto, T. Yagi, Y. Hikichi, Y. Suematsu, T. Yamamoto**Optimal kissing balloon inflation after single-stent deployment in a coronary bifurcation model**

Eurointervention, 10 (2014), pp. 934-941

[23]

S. Rahman, T. Leesar, M. Cilingiroglu, M. Effat, I. Arif, T. Helmy, *et al.***Impact of kissing balloon inflation on the main vessel stent volume, area, and symmetry after side-branch dilation in patients with coronary bifurcation lesions: a serial volumetric intravascular ultrasound study**

JACC Cardiovasc Interv, 6 (2013), pp. 923-931

[24]

G. Rigatelli, F. Dell'Avvocata, M. Zuin, S. Giatti, K. Duong, T. Pham, *et al.***Comparative computed flow dynamic analysis of different optimization techniques in left main either provisional or Culotte stenting**

J Transl Int Med, 5 (2017), pp. 205-212

[25]

F. Derimay, G. Souteyrand, P. Motreff, G. Rioufol, G. Finet**Influence of platform design of six different drug-eluting stents in provisional coronary bifurcation stenting by rePOT sequence: a comparative bench analysis**

EuroIntervention, 13 (2017), pp. e1092-e1095

[26]

E. Romagnoli, L. Gatto, A. La Manna, *et al.***Role of residual acute stent malapposition in percutaneous coronary interventions**

Catheter Cardiovasc Interv, 90 (2017), pp. 566-575

[27]

T. Gori, A. Polimeni, C. Indolfi, L. Räber, T. Adriaenssens, T. Münzel**Predictors of stent thrombosis and their implications for clinical practice**

Nat Rev Cardiol, 16 (2019), pp. 243-256

[28]

D. Mitsouras, P. Liacouras, A. Imanzadeh, *et al.***Medical 3D printing for the radiologist RadioGraphics; Antoniadis et al. Biomechanical modeling to improve coronary artery bifurcation stenting: expert review document on techniques and clinical implementation**

JACC (2015)

[29]

F. Morlacchi**Migliavacca Modeling stented coronary arteries: where we are, where to go**

Ann Biomed Eng, 41 (2013), pp. 1428-1444

[30]

K. Toutouzas, Y.S. Chatzizisis, M. Riga, *et al.***Accurate and reproducible reconstruction of coronary arteries and endothelial shear stress calculation using 3D OCT: comparative study to 3D IVUS and 3D QCA**

Atherosclerosis, 240 (2015), pp. 510-519

[31]

F. Dérimay, G. Rioufol, T. Nishi, Y. Kobayashi, W.F. Fearon, J. Veziers, *et al.***Optimal balloon positioning for the proximal optimization technique? An experimental bench study**

Int J Cardiol, 292 (2019), pp. 95-97

Tables

Table 1. Comparison of the three different proximal optimization techniques (POTs) after the cross-over stenting technique; SBO: side branch occlusion. *p<0.05 compared to traditional POT.

	Standard POT N=5	**Proximal POT N=5**	**Distal POT N=5**
LM			
D_{ref} (mm)	4.11±0.05	4.06±0.06	4.09±0.04
$D_{scaffold/stent}$ (mm)	4.29±0.04	4.11±0.04	4.20±0.05
Stent/artery ratio	1.04±0.03	1.01±0.05	1.02±0.05
LAD			
D_{ref} (mm)	3.28±0.05	3.14±0.03	3.31±0.04
$D_{scaffold/stent}$ (mm)	3.40±0.03	3.34±0.08	3.60±0.02
Stent/artery ratio	1.03±0.02	1.06±0.05	1.08±0.03
LCX			
D_{ref} (mm)	2.94±0.03	2.86±0.05	2.90±0.04
SBO (%)	18.3±3.6	38.3±5.1 *	29.3±3.1 *
Global stent malapposition	7/1135	18/1135	9/1135
	0.78±1.2	1.3±0.4 *	0.82±1.8

Table 2. Elliptical ratio among the different proximal optimization technique configurations used in the analysis.

	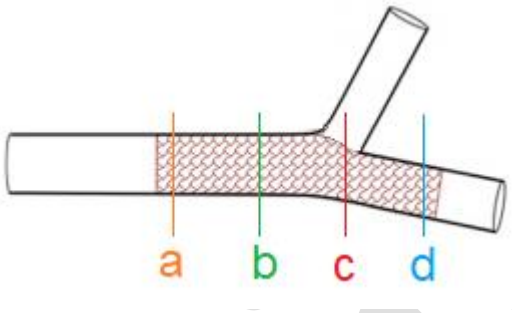		
Sites	**Standard POT** **N=5**	**Proximal POT** **N=5**	**Distal POT** **N=5**
A	1.01±0.01	0.80±0.02	1.01±0.02
B	1.00±0.02	0.70±0.04	0.88±0.03
C	0.75±0.04	0.60±0.03	0.80±0.02
D	0.98±0.02	1.02±0.02	0.92±0.03

Figures

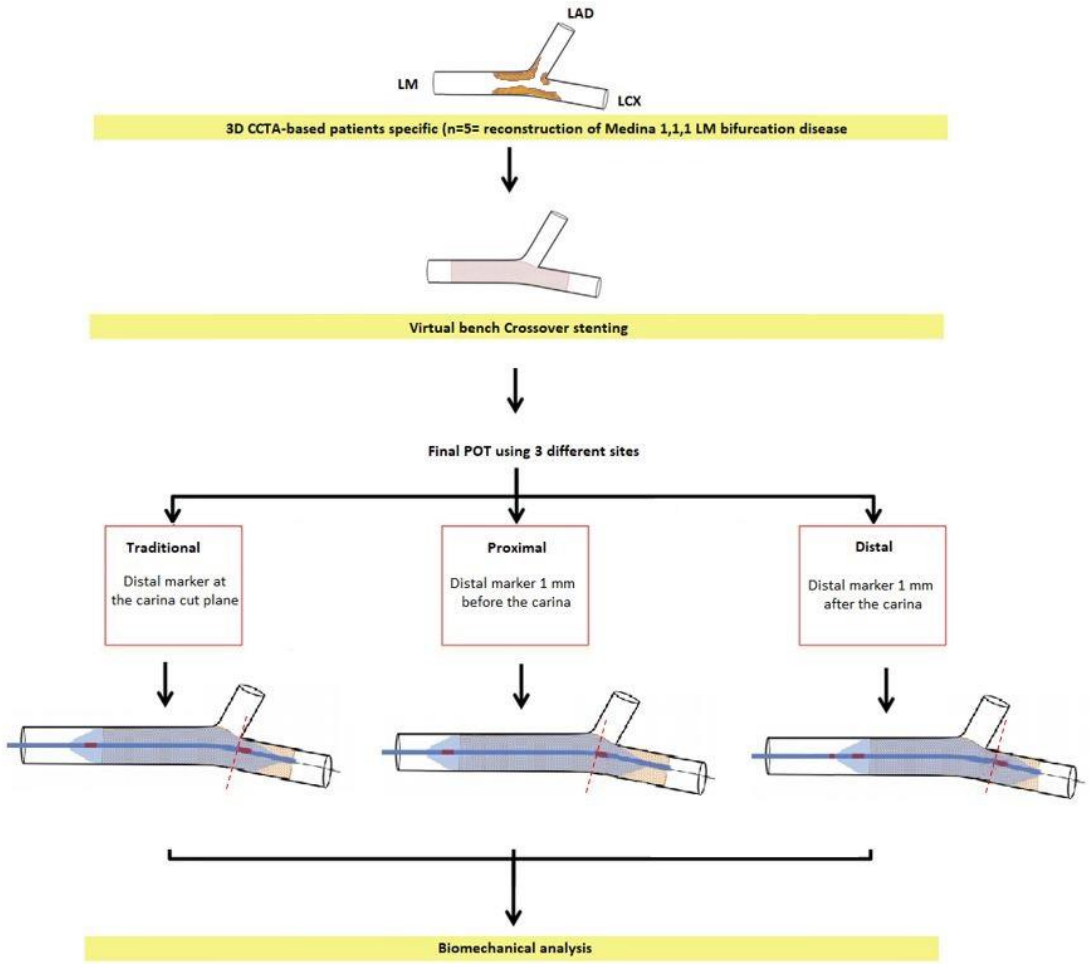

Figure 1. Flow chart of the study. LM: left main; LAD: left anterior descending; LCX: left circumflex; CCTA: cardiac computed tomography angiography; POT: proximal optimization technique.

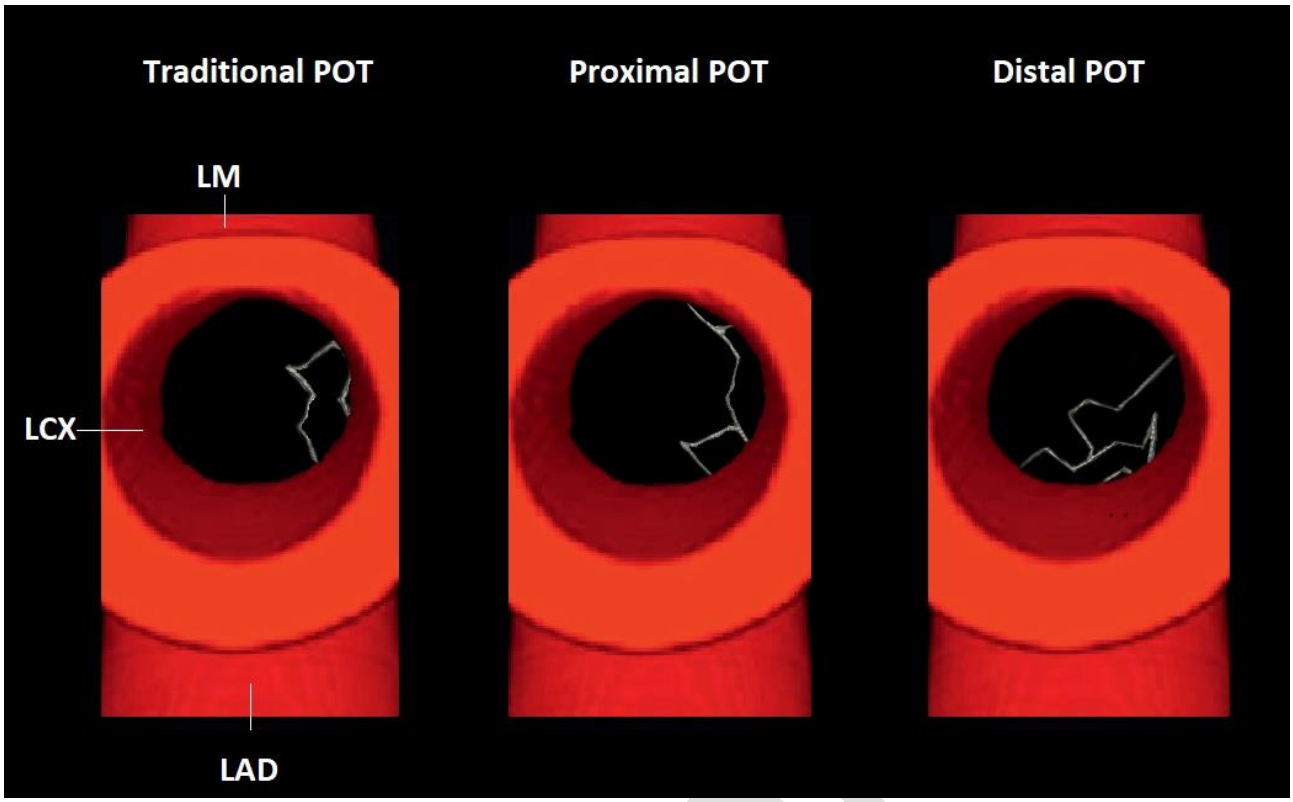

Figure 2. View of the ostium from the SB after simulating the final proximal optimization technique (POT) in a 54-year-old diabetic male patient, demonstrating a different involvement of the ostial opening related to the different POT strategies used. LAD: left anterior descending coronary artery; LCX: left circumflex artery.